CHE 7916324, is also gratefully acknowledged. V.C.G. acknowledges support from a NATO Postdoctoral Fellowship administered through the Science and Engineering Research Council, U.K.

Supplementary Material Available: Tables of spectral (^{1}H NMR, ^{13}C NMR, IR, mass spectrum) and microanalytical data (4 pages). Ordering information is given on any current masthead page.

Solvent Control of Oxidation State Distribution and Electronic Delocalization in an Osmium–Ruthenium, Mixed-Metal Dimer

Joseph T. Hupp, Gregory A. Neyhart, and Thomas J. Meyer*

Department of Chemistry
The University of North Carolina
Chapel Hill, North Carolina 27514
Received January 9, 1986

In mixed-valence dimers the position and extent of delocalization of the odd electron depends on the metals and on the bridging and nonbridging ligands.[1] We report here the preparation of the mixed-metal dimer $[(bpy)_2(Cl)Os^{II}(pz)Ru^{II}(NH_3)_5]^{3+}$ (bpy is 2,2′-bipyridine; pz is pyrazine) in which the metal–ligand combinations at the two sites lead to redox potentials for the $Os^{III/II}$ and $Ru^{III/II}$ couples which are nearly of the same magnitude.[2,3] However, because of a considerable difference in the sensitivity of the potentials of the two couples to solvent,[4] we have been able to demonstrate that in the mixed-valence form of the dimer, intramolecular electron transfer can be induced by changes in the solvent. Perhaps more interestingly, we also find that variations in solvent appear to affect the extent of delocalization of the odd electron.

In acetonitrile at μ = 0.1 M, reversible $E_{1/2}$ values (cyclic voltammetry) for the two metal-based redox couples in the dimer occur at +0.38 and +0.01 V vs. ferricinium/ferrocene as an internal reference (+0.72 and +0.35 vs. the saturated sodium calomel electrode).

$$M^{III}(L)M'^{II} + e^- \rightarrow M^{II}(L)M'^{II}; \quad E_{1/2}(1) \qquad (1)$$

$$M^{II}(L)M'^{II} + e^- \rightarrow M^{II}(L)M'^{I}; \quad E_{1/2}(2) \qquad (2)$$

The large potential difference between the III,III/II,III and II,III/II,II couples, $E_{1/2}$ (1) − $E_{1/2}$ (2), arises chiefly from electrostatic and electronic coupling effects.[1,3] One-electron oxidation gives the mixed oxidation state dimer $M^{II}(L)M'^{III}$. From the UV–visible spectra of the mixed oxidation state dimer, the reduced dimer, and the related monomers (Figure 1) the oxidation state distribution within the dimer in nitromethane is $[(bpy)_2(Cl)Os^{III}(pz)Ru^{II}(NH_3)_5]^{4+}$ and in dimethylformamide it is $[(bpy)_2(Cl)Os^{II}(pz)Ru^{III}(NH_3)_5]^{4+}$. On going from the monomer

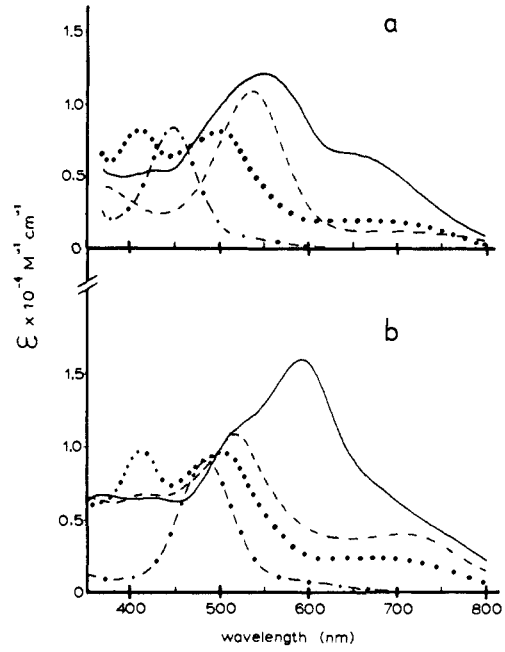

Figure 1. UV–visible absorption spectra in (a) nitromethane and (b) dimethylformamide, for $[Ru^{II}(NH_3)_5(pz)]^{2+}$ (---), $[(bpy)_2(Cl)Os^{II}(pz)]^{+}$ (···), $[(bpy)_2(Cl)Os(pz)Ru(NH_3)_5]^{4+}$ (- - -), and $[(bpy)_2(Cl)Os(pz)Ru(NH_3)_5]^{5+}$ (—).

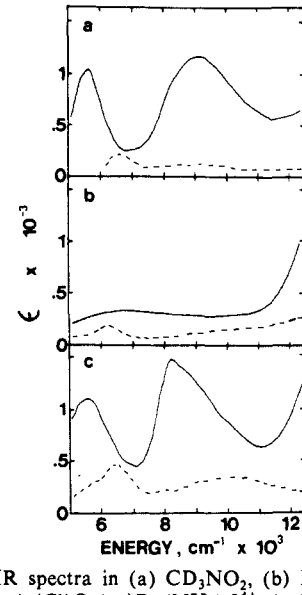

Figure 2. Near-IR spectra in (a) CD_3NO_2, (b) Me_2SO-d_6, and (c) CD_3CN, for $[(bpy)_2(Cl)Os(pz)Ru(NH_3)_5]^{4+}$ (—) and $[(bpy)_2(Cl)Os^{III}(pz)Ru^{III}(NH_3)_5]^{5+}$ (- - -).

to the dimer in nitromethane, the shift in the $d\pi[Ru^{II}(NH_3)_5] \rightarrow \pi^*(pz)$ transition from 436 to 534 nm is expected because of stabilization of $\pi^*(pz)$ by binding at the remote nitrogen of the ligand bridge.[4a,5] In dimethylformamide, the multiple $d\pi(Os^{II}) \rightarrow \pi^*$ (bpy) transitions associated with Os(II) appear and the intense band at 720 nm arises from a $d\pi(Os^{II}) \rightarrow \pi^*$ (pz) transition. Also noteworthy is the loss of the highest $d\pi \rightarrow \pi^*$ transition (420 nm) upon dimer formation; this appears to be a general property of pyrazine-bridged Os(II) dimers.

The equilibrium between oxidation state isomers in reaction 3 can be perturbed by variations in the solvent. Spectral studies

$$[(bpy)_2(Cl)Os^{III}(pz)Ru^{II}(NH_3)_5]^{4+} \rightleftharpoons [(bpy)_2(Cl)Os^{II}(pz)Ru^{III}(NH_3)_5]^{4+} \qquad (3)$$

show, for example, that the addition of Me_2SO to CH_3NO_2 so-

(1) (a) Creutz, C. *Prog. Inorg. Chem.* **1983**, *30*, 1. (b) Meyer, T. J. In *Mixed Valence Compounds*; Brown, D. B., Ed.; D. Reidel: Dordrecht, Holland, 1980; pp 75–113.

(2) The salt $[(bpy)_2(Cl)Os(pz)Ru(NH_3)_5](PF_6)_3$ was prepared by using the procedure described for the analogous Ru–Ru complex (Callahan, R. W.; Brown, G. M.; Meyer, T. J. *Inorg. Chem.* **1975**, *14*, 1443). Equimolar amounts of the solids $[(bpy)_2(Cl)Os(pz)](PF_6)$ and $[Ru(NH_3)_5(OH_2)](PF_6)_2$ were added to a deaerated 50-mL Erlenmeyer flask. Deaerated acetone was added by syringe and the mixture was stirred in the absence of light under a blanket of Ar for 1 h. The dimeric PF_6^- salt was precipitated by adding the reaction mixture dropwise into 100 mL of stirring dichloromethane. The resulting solid was collected and purified by reprecipitation from acetone/ether followed by stirring in dichloromethane to remove monomeric impurities. Anal. Calcd for $[(bpy)_2(Cl)Os(pz)Ru(NH_3)_5](PF_6)_3 \cdot 2H_2O$: C, 22.6%; H, 3.09; N, 12.08. Found: C, 20.43; H, 3.04; N, 12.08. The 4+ and 5+ dimers were prepared in situ by using Br_2 as oxidant.

(3) Hupp, J. T.; Curtis, J. C.; Neyhart, G. A., unpublished results.

(4) (a) Powers, M. J.; Callahan, R. W.; Salmon, D. J.; Meyer, T. J. *Inorg. Chem.* **1976**, *15*, 1457. (b) Chang, P. C.; Fung, E. Y.; De la Rosa, R.; Curtis, J. C., manuscript in preparation. (c) Hupp, J. T.; Weaver, M. J. *J. Phys. Chem.* **1985**, *89*, 2787.

(5) Creutz, C.; Taube, H. *J. Am. Chem. Soc.* **1969**, *91*, 3988; **1973**, 95, 1086.

0002-7863/86/1508-5349$01.50/0

lutions containing the mixed oxidation state dimer shifts eq 3 in favor of the $Os^{II}(L)Ru^{III}$ isomer. From spectral studies, Os^{II}-$(pz)Ru^{III}$ is slightly the predominant isomer in CH_3CN, but the two forms coexist and $\Delta G \sim 0$ for reaction 3.[6]

As in related mixed-valence dimers,[1,4a,b,5,7] metal-to-metal charge-transfer (MMCT) bands appear in near-IR spectra of the mixed oxidation state dimer as shown in Figure 2 for CD_3NO_2, CD_3CN, and Me_2SO-d_6 as solvent. The origin of the relatively broad band ($\Delta\bar{\nu}_{1/2} = 1.3 \times 10^3$ cm^{-1} at $E_{max} = 9.0 \times 10^3$ cm^{-1}) in nitromethane is the MMCT transition.[8]

$$[(bpy)_2(Cl)Os^{III}(pz)Ru^{II}(NH_3)_5]^{4+} \xrightarrow{h\nu} [(bpy)_2(Cl)Os^{II}(pz)Ru^{III}(NH_3)_5]^{4+} \quad (4)$$

This band is somewhat narrower than commonly observed in localized mixed-valence dimers. The narrow band in Figure 2a at $\sim 5.6 \times 10^3$ cm^{-1} arises from the second of an expected two $d\pi \rightarrow d\pi$ spin–orbit transitions based on the d^5 Os^{III} site[7,9] and is a useful oxidation state marker. The transition appears in the Os^{III} monomer and $Os^{III}(pz)Ru^{II}$ dimer but not in the $Os^{II}(pz)Ru^{II}$ dimer nor in the mixed oxidation state dimer in Me_2SO-d_6 (Figure 2b). In Me_2SO, UV–visible spectra show that the oxidation state distribution is $Os^{II}(pz)Ru^{III}$ and the MMCT band arises from the transition.

$$[(bpy)_2(Cl)Os^{II}(pz)Ru^{III}(NH_3)_5]^{4+} \xrightarrow{h\nu} [(bpy)_2(Cl)Os^{III}(pz)Ru^{II}(NH_3)_5]^{4+} \quad (5)$$

The MMCT band has the broad featureless character of the reverse transition in CD_3NO_2 but is less intense and somewhat distorted by an underlying absorption feature at higher energy. An absorption increase for the $Os^{III}(L)Ru^{III}$ dimer below 5000 cm^{-1} (not shown) arises because of the onset of the lower energy of the two $d\pi \rightarrow d\pi$ transitions based at Os(III).

The low-energy absorption spectrum of the mixed oxidation state dimer in CD_3CN (Figure 2c) has some distinctive features when compared with the spectra in CD_3NO_2 or Me_2SO-d_6. The availability of a wider solvent spectral window allows both Os^{III} based spin–orbit bands to be observed, the lower at $E \leq 3.6 \times 10^3$ cm^{-1} and the higher, which appears in Figure 2c, at 5.6×10^3 cm^{-1}. Of more interest is the fact that the MMCT band becomes noticeably asymmetric, in a fashion somewhat reminiscent of the MMCT band for the Creutz and Taube ion, $[(NH_3)_5Ru(pz)$-$Ru(NH_3)_5]^{5+}$.[1,5,10]

The results presented here show that variations in solvent can be used to control the oxidation state distribution within the Os–Ru mixed oxidation state dimer and, thus, to induce intramolecular electron transfer. The change in band shape in acetonitrile (which is *not* observed in the analogous dimer with 4,4′-bipyridine as the bridge) suggests that *the nature of the electronic delocalization between metals can be influenced by solvent variations* as well. A possible microscopic origin for the solvent effect is suggested by the spectral data. In CH_3CN, ΔG approaches zero for intramolecular electron exchange (eq 3). The combination of $\Delta G \sim 0$, moderate electronic coupling across pyrazine, and relatively low vibrational trapping barriers[1] may lead to thermal intramolecular electron transfer rates which approach or even exceed the time scale of solvent dipole reorientations, 10^{-11}–10^{-12} s.[11] An exchange process in this time domain would diminish the ability of the solvent dipoles to trap the exchanging electron at a single site and explain the change in band shape for the MMCT band as arising from a partly "relaxed" solvent dipole environment around the ion. In nitromethane or Me_2SO, ΔG is positive for intramolecular electron transfer (either $Ru^{II} \rightarrow Os^{III}$ or $Os^{II} \rightarrow Ru^{III}$). In these solvents electron transfer may be slow compared to the time scale for solvent dipole reorientations, giving rise to the full width and symmetrical band shape expected for a MMCT transition in a "localized" dimer.[8]

Acknowledgments are made to Jeff Curtis for stimulating discussions and to the US Army Research Office—Durham under Grant DAAG29-85-K-0121 and the National Science Foundation under Grant CHE-8503092 for support of this research.

(6) Because of the large potential difference between $E_{1/2}(1)$ and $E_{1/2}(2)$, 0.37 V in CH_3CN, disproportionation, $2[(bpy)_2(Cl)Os(pz)Ru(NH_3)_5]^{4+} \rightarrow [(bpy)_2(Cl)Os^{III}(pz)Ru^{III}(NH_3)_5]^{5+} + [(bpy)_2(Cl)Os^{II}(pz)Ru^{II}(NH_3)_5]^{3+}$, is disfavored by $\sim 10^6$ and cannot be the origin of the appearance of transitions associated with Ru^{II} in the spectrum.

(7) Kober, E. M.; Goldsby, K. A.; Narayana, D. N. S.; Meyer, T. J. *J. Am. Chem. Soc.* **1983**, *105*, 4303.

(8) Hush, N. S. *Prog. Inorg. Chem.* **1967**, *8*, 391.

(9) Sen, J.; Taube, H. *Acta Chem. Scand., Ser. A* **1979**, *33*, 125.

(10) Furholz, U.; Burgi, H-B; Wagner, F. E.; Stebler, A.; Ammeter, J. H.; Krausz, E.; Clark, R. J. H.; Stead, M. J.; Ludi, A. *J. Am. Chem. Soc.* **1984**, *106*, 121.

(11) See, for Example: Calef, D. F.; Wolynes, P. G. *J. Phys. Chem.* **1983**, *87*, 3387.

Charge Separation and Energy Transfer in Carotenopyropheophorbide–Quinone Triads

Paul A. Liddell, Donna Barrett, Lewis R. Makings, Peter J. Pessiki, Devens Gust,* and Thomas A. Moore*

Department of Chemistry, Arizona State University Tempe, Arizona 85287

Received January 31, 1986

In natural photosynthetic membranes, chlorophyll molecules serve as the site of the initial photodriven charge separation. In addition, they play a role in subsequent electron-transfer steps, accept singlet excitation energy from carotenoid antenna molecules, and transfer triplet energy to carotenoid acceptors (thereby preventing sensitized singlet oxygen production and subsequent photodamage to the organism). We report herein the synthesis and study of chlorophyll-based carotenopyropheophorbide–quinone triad molecules which mimic all of these natural processes. Irradiation of **1** in solution initiates a two-step electron transfer

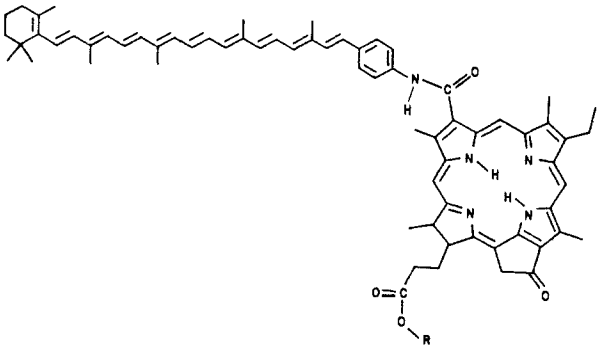

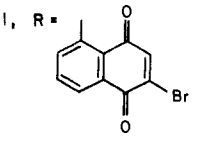

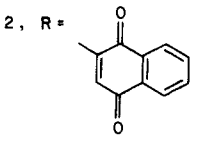

leading to the formation of an energetic charge-separated state with a quantum yield of ca. 4% and a lifetime of 120 ns. Carotenopyropheophorbide **3** demonstrates singlet–singlet energy transfer from the carotenoid moiety to the pyropheophorbide with 50% efficiency. The carotenoid moiety of **3** also provides photoprotection from singlet oxygen formation by quenching the pyropheophorbide triplet state within 50 ns of its formation.

The syntheses of **1** and **2** were achieved by coupling 2-devinyl-2-(carboxymethyl)pyropheophorbide *a* to the appropriate aminocarotenoid via the acid chloride to yield **3**, cleaving the methyl ester with potassium carbonate and esterifying with 2-bromojuglone or lawsone, respectively. Information concerning the solution conformations of **1**–**3** was deduced from 400-MHz ^{1}H NMR spectra by analyzing[1] tetrapyrrole aromatic-ring-cur-

0002-7863/86/1508-5350$01.50/0